Non-Toxic Auxiliary Propulsion System Modeling of Liquid Oxygen Tank and Accumulator for Ground Tests

Kevin Miller
Eric Hurlbert
NASA Johnson Space Center
Houston, TX 77058

Abstract

A thermal & fluid analysis of a liquid oxygen tank and feedsystem is being performed to support non-toxic propulsion system ground test bed activities. The test bed is to demonstrate the technologies required for implementing a liquid oxygen and ethanol auxiliary propulsion system. The cryogenic tank and accumulator were modeled using the SINDA/FLUINT thermal/fluid network analyzer. The objectives of the analysis are to determine loading and chilldown timelines in order to meet a one-hour maximum time allotted to complete loading 4600 lbm of LOX into the tank, feedlines and accumulator. The results determined the orifice sizes required to vent the boil-off and the effect of orientation on the bellows accumulator thermal response. The model was used to establish the feasibility of meeting the 1-hour loading time requirement. The current model might be further developed to include all phases of test bed system operation including multiple thruster firings and long quiescent periods.

Nomenclature

APS – Auxiliary Propulsion System
FBC – full boiling curve method
GHe – gaseous helium
GOX – gaseous oxygen
JSC – Johnson Space Center
LOX – liquid oxygen
NASA – National Aeronautics & Space Administration
NT – Non-Toxic
QMAX – critical heat flux method
TB – Test Bed
SINDA/FLUINT – Systems Improved Numerical Differencing Analyzer with Fluid Integrator

Bo – Bond number, $g (\rho_l - \rho_v) L^2 / \sigma$
Cd – valve discharge coefficient
Cv – valve flow coefficient
Gr – Grashof number, $g \beta (T_s - T_l) L^3 / \nu^2$
Ja – Jakob number, $c_p (T_s - T_{sat}) / h_{fg}$
L – characteristic length
Nu – Nusselt number, $h L / k$
Pr – Prandtl number, $c_p \mu / k$
Ra – Rayleigh number, Pr x Gr
Re – Reynolds number, $\rho V L / \mu$
T – temperature
ΔT_{excess} – excess temperature
V – flow velocity

c_p – specific heat at constant pressure
g – gravitational acceleration
h – heat transfer film coefficient
h_{fg} – heat of vaporization
k – thermal conductivity
q" – heat flux

β – volumetric thermal expansion coefficient
μ – viscosity
ν – kinematic viscosity
ρ – density
σ – surface tension or Stefan-Boltzmann constant

Subscripts:

l – liquid
v – vapor
s – wall, metal surface
sat – saturation
b – boiling
r – radiation
max – maximum, critical value
min - minimum

Introduction

The Non-Toxic Auxiliary Propulsion System Test Bed (NT-APS-TB) will address many important aspects of an on-orbit cryogenic propulsion system. The test bed objectives are to:

a) Demonstrate safe and reliable operation
b) Test multiple dual thrust engines
c) Demonstrate igniter capabilities
d) Demonstrate quiescent operation of system with and without active thermal conditioning of lines
e) Test feedsystem insulation and thermal conditioning method(s)
f) Test different line configurations to anchor math models with data
g) Demonstrate rapid loading, flight, landing, and turnaround operations
h) Demonstrate integrated vehicle health management that operates system autonomously
i) Accumulate life and cycles on hardware to demonstrate reliability

The test bed can be configured in either a short or long configuration. The short configuration consists of 10 ft of feedline running to the thruster manifolds. This setup simulates propellant distribution in the aft of a flight vehicle. The long configuration includes 225 ft of feedline and a propellant accumulator upstream of the thrusters in order to simulate propellant distribution from the aft of a flight vehicle to the forward ACS thrusters.

Characterizing the thermal performance of a cryogenic system is a key to implementing an on-orbit APS. To this end, efforts have begun to mathematically model the NT-APS-TB LOX system. This analysis described in this paper begins to address test bed thermal performance. Eventually, thermal models will be anchored to test data from various duty cycles/mission profiles in order to characterize the system.

Cryogenic Feedsystem Chilldown

The liquid oxygen side of the feedsystem must be chilled down from ambient temperatures (~540°R) to cryogenic temperatures (~160°R) in one hour. System chilldown is accomplished by flowing LOX into the feedline via a single facility fill line and venting the attendant boil-off. The facility fill line connects to the feedsystem just below the propellant tank outlet. Venting occurs through three vent valves: the tank vent valve and two valves on the two thruster manifolds. The NT-APS-TB fluid system is shown schematically in Figure 1.

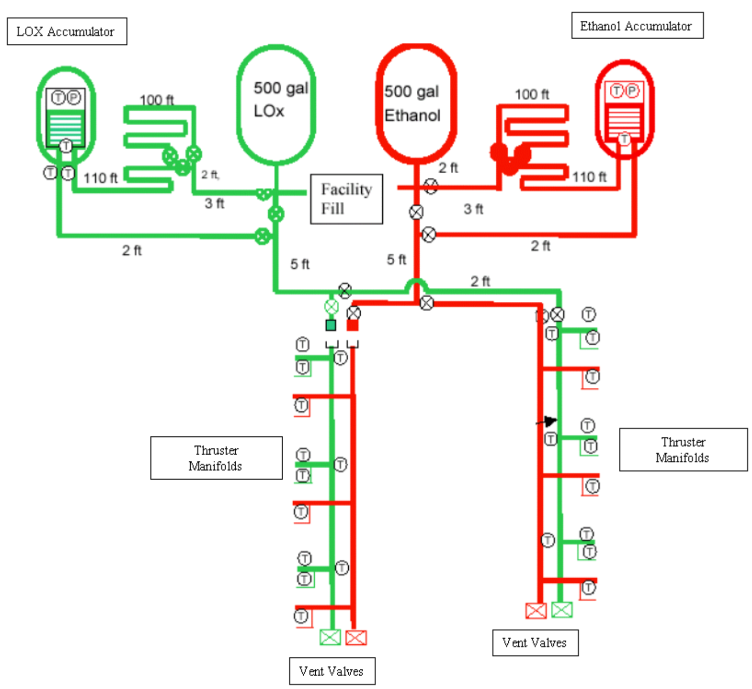

Figure 1: Non-Toxic Auxiliary Propulsion System Test Bed fluid system schematic

The flow quality at a given point along the feedline, as well as the flow split between the tank and feedlines will shift throughout the chilldown process. System pressures will also vary with LOX inflow rate and thermal resistance. Some modeling simplifications were made in order to analyze the chilldown responses of the accumulator and tank separately. These simplifications will be explained further in their respective sections.

LOX Accumulator

The fuel and oxidizer feedlines both utilize a bellows accumulator when the system is operating in the forward (long) configuration. The accumulators are used to dampen pressure transients associated with pulsing thrusters and may also be isolated from the propellant tank and operated in blow-down mode to simulate various mission scenarios.

The accumulator design consists of a single concentric inlet/outlet port for LOX flow-through and is loaded on the backside (ullage side) with GHe. A fixed mass of GHe is loaded in the ullage prior to test operations so that the nominal propellant load will be contained in the accumulator at thermal and pressure equilibrium. The ullage gas and accumulator hardware must cool down in order to load the accumulator fully.

Preliminary dynamic analysis of the feedsystem set the accumulator LOX load at 1800 in^3 for nominal feedline conditions of 350 psia and 163°R. A schematic of the accumulator is shown in Figure 2.

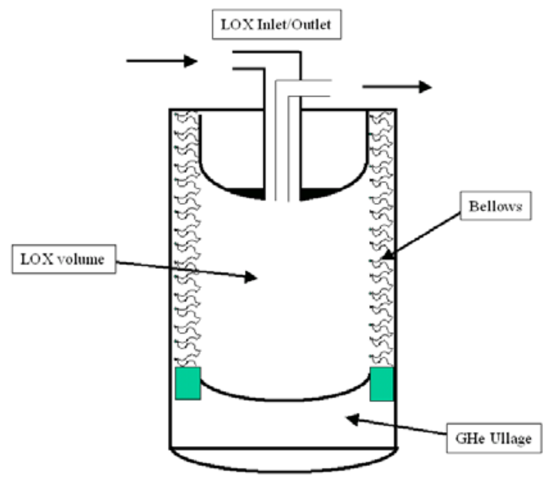

Figure 2: LOX Accumulator

Accumulator Modeling

The accumulator diameter and total volume were design variables examined in the chilldown analysis. Four accumulator sizes were modeled and their characteristics are listed in Table 1.

Design	A2	A4	B2	B4
Internal Diameter, (in)	8.2	8.2	12	12
Wall Thickness, (in)	0.125	0.125	0.250	0.250
Nominal LOX Volume (in^3)	1800	1800	1800	1800
Ullage Volume, (in^3)	200	400	200	400
Total Volume, (in^3)	200	2200	2000	2200
Accumulator Mass (lbm)	39	43	66	71
Length, (in)	37.9	41.7	17.7	19.5
Stroke, (in)	34.3	34.3	16	16
Bellows Spring Rate, (lbf/in)	100	100	100	100

Table 1: Accumulator sizing comparison

Another design option considered in this analysis was the orientation of the accumulator. The accumulator could be vertically aligned so that the GHe-side was above the LOX-side or vice versa. Heat transfer is inherently different for each orientation due to the orientation of the temperature gradient with respect to the force of gravity.

Initially, the accumulator will see oxygen vapor and two-phase flow as the upstream plumbing is being chilled. After sufficient cooling is reached upstream of the accumulator, liquid will start to flow through the accumulator and the bellows will expand as system pressure rises. The bellows will continue to expand as the accumulator hardware and GHe ullage is cooled down. For the purposes of the accumulator chilldown analysis, the chilldown of the feedlines and accumulator were assumed to occur separately and in series. Feedline chilldown has not been included in the system modeling effort to this point; therefore the accumulator analysis starts with the assumption of a chilled and pressurized feedline and concludes when the bellows has been loaded with a sufficient amount of LOX. The expected time required to chill the feedlines is then added to the accumulator loading time.

A thermal/fluid model of the accumulator was created using SINDA/FLUINT. The fluid submodel consists of two tanks connected via an *IFACE* macro used to balance the forces on the bellows cap and simulate the spring-like behavior of the bellows. The accumulator thermal model consists of eight diffusion nodes that take into consideration the thermal mass of the accumulator body and a single diffusion node that represents the cap of the bellows. The accumulator thermal model is shown in Figure 3.

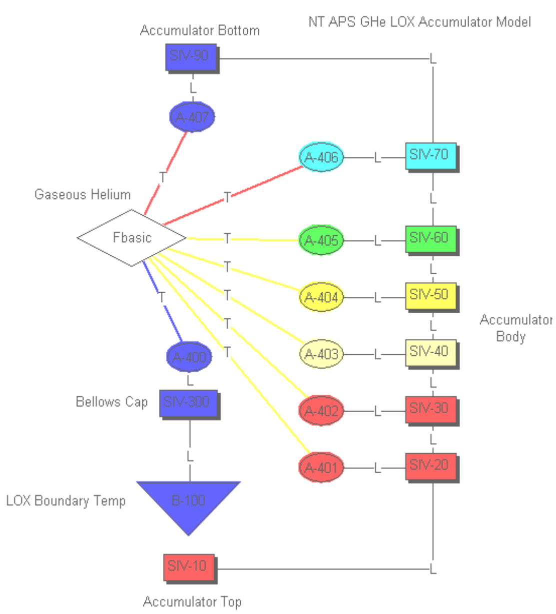

Figure 3: Accumulator Thermal Model

The thermal and fluid models are tied together via user-defined heat transfer (*HTU*) ties. Film coefficients are solved accordingly for gas conduction or free convection, depending on which method (orientation) is selected. Ties are also attached or disconnected depending on the position of the bellows, thereby making convection heat transfer area a function ullage volume.

The assumption of a chilled feedline sets the cold wall boundary temperature at 163°R placed on the LOX side of the bellows. Heat leaks due to support penetrations, the GHe charge line, and radiation are imposed upon the accumulator body.

Chilldown runs are carried out in three steps:

1) The appropriate amount of GHe to ensure nominal LOX volume is loaded into the ullage

2) The ullage is adiabatically compressed from the LOX feedline pressure acting against the other side of the bellows cap

3) Heat transfer between the fluids and the metal is enabled

Two orientations of the accumulator were modeled by using two different dominant modes of heat transfer. The differences in the two heat transfer models are explained below.

<u>GHe-above-LOX</u>:

In this orientation, stratification of the ullage gas is assumed. Heat is transferred from the accumulator body and bellows cap to the ullage solely by gas conduction, therefore Nu = 1. No convection currents are able to set up in the ullage as dictated by the temperature gradient.

<u>LOX-above-GHe</u>:

Heat transfer is augmented in the ullage volume by free convection currents. Warm GHe rises to the top where it is cooled through the bellows cap and then descends back into the warmer ullage to pick up more heat from the accumulator body. Free convection heat transfer through the circular bellows cap and accumulator end wall are correlated using [1]:

$$Nu = 0.15 Ra^{1/3} \tag{1}$$

Heat transfer to the accumulator sidewalls is defined in the limit of laminar flow [2]:

$$Nu = 3.66 \tag{2}$$

The difference between the two orientations was much more drastic in the chill down of the accumulator than any of the sizing design variables.

Accumulator Model Results & Analysis

Chilldown analyses of the two proposed accumulator orientations were performed to compare the effectiveness of the two heat transfer modes. Results of this comparison are shown in Figures 4 & 5. Design Type-A2 was used for the accumulator size to generate the output in both plots. All modeling output was plotted using EZ-XY plotting software.

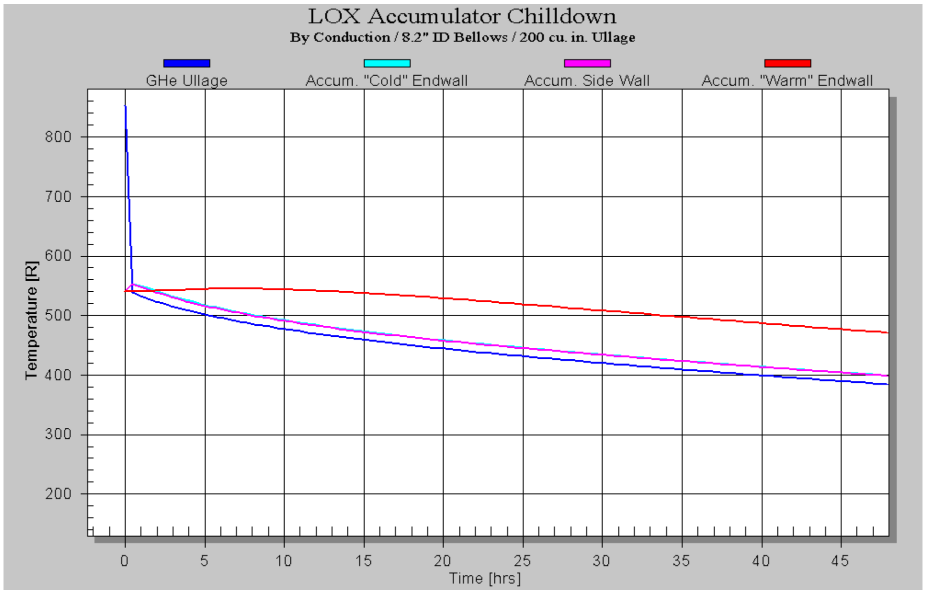

Figure 4: GHe-above-LOX orientation chilldown profile

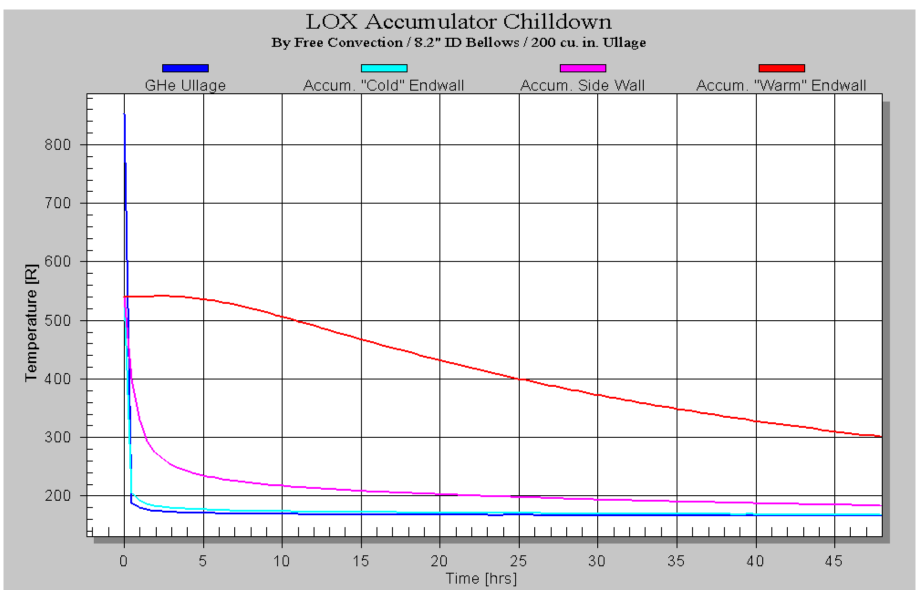

Figure 5: LOX-above-GHe orientation chilldown profile

The two orientations exhibited vastly different chilldown rates. The LOX-above-GHe orientation shows all temperatures falling off quicker than the GHe-above-LOX orientation. Most importantly, the GHe ullage temperature comes down rapidly in the free convection model, which translates into a quicker loading of the accumulator. The ullage temperature starts at approximately 850ºR due to the adiabatic compression assumption of the ullage to feedline pressure. The accumulator "warm" end wall exhibits a slow chilldown rate in Figure 5 on the order of 7-15 ºR/hr. The accumulator "warm" end wall (end opposite of ullage) is isolated from any fluid in the model and cools only through solid conduction to the "cold" end wall (end wetted by ullage gas). The conduction path between the "warm" and "cold" end walls is long owing to the slow cool down rate compared to temperatures on the ullage end of the accumulator.

The modeling results from Figures 4 & 5 lent more interest to the LOX-above-GHe orientation. A sizing comparison was carried out for this arrangement, as accumulator dimensions were not yet determined by the system dynamic analysis. The results of the sizing comparison are shown in Figure 6 below.

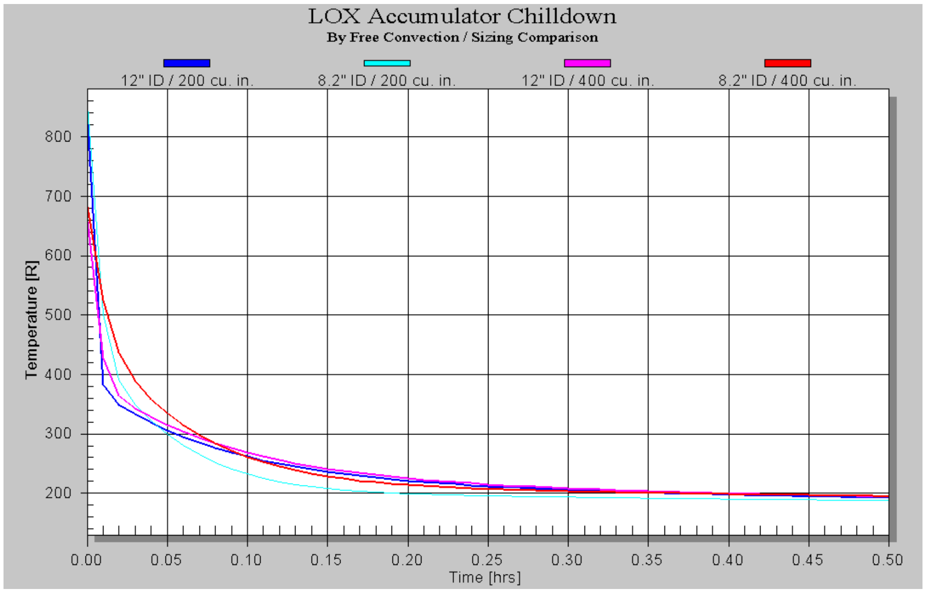

Figure 6: Ullage Chilldown Sizing Comparison

The initial ullage temperatures differ between the two nominal ullage volumes due to the 200-in^3 design (Type-2) experiencing more compression than the 400-in^3 design (Type-4). The chilldown trends between the 8.2-in diameter (Type-A) and the 12-in diameter (Type-B) are also distinctly different. The Type-A accumulator is longer and has thinner walls than Type-B. This owes to a larger resistance to conductive heat transfer from the warm end wall to the cold end wall. Since heat is transferred at a slower rate to the ullage end of the accumulator in Type-A, the ullage temperature initially comes down at a quicker rate than in the Type-B design in the chilldown transient analysis.

Under the 163ºR LOX cold-wall boundary assumption, the accumulator cannot reach full loading, but only approach it as the ullage is cooled to LOX temperature. For this reason, chilldown times are given in terms of 90% and 95% of full LOX loading times, which correspond to 1620 in^3 and 1710 in^3 of LOX, respectively. The loading times are given in Table 2.

Design	90% load time (min)	95% load time (min)
A2	3	6
A4	8	28
B2	3	10
B4	11	29

Table 2: Accumulator load times

All accumulator designs load up to 95% within one-half hour. Data from recent cryogenic testing at NASA/JSC is used as the basis for estimating possible feedline chilldown times. Drawing from this experience, it is expected that the NT-APS-TB feedlines will be able to chill down within one-half hour. Analysis indicates that the one-hour requirement is feasible under the present assumption that the feedlines and accumulator chill down separately.

LOX Propellant Tank

The 61-in diameter LOX tank has 0.312" thick walls and is suspended inside a vacuum chamber. The tank is wrapped with 100 layers of MLI to lower radiation heat transfer to meet long duration tests. System requirements call for the propellant tank to be loaded with up to 4400 lbm of liquid oxygen while achieving 80-85 ºR of subcooling at 350 psia. A drawing of the tank is shown in Figure 7.

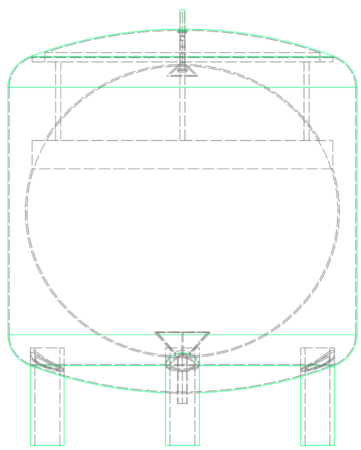

Figure 7: Liquid Oxygen Tank

The tank is chilled in parallel with the rest of the feedsystem. The LOX tank is loaded up through the bottom of the tank. Cooling of the tank is done primarily through boiling of saturated liquid upon entering the tank. Heat is also transferred from the tank metal via convection as the oxygen vapor is flowed out of the tank. Oxygen boil-off is vented through a single valve located at the top of the tank. Tank pressure will rise depending on the boil-off rate and the vent valve flow capacity. A chilldown analysis was performed on the tank to investigate important system design parameters such as vent valve sizing and loading profiles.

Tank Modeling

A single *twinned tank* lump is used to model the filling of the LOX tank. The *twinned tank* lump allows for simplified handling of heat and mass transfer across a non-homogenous liquid/vapor interface.

A *CTLVLV* (control valve) macro is used in line with a plenum and a lump to model upstream LOX conditions prior to entry into the tank. The lump represents the volume of the short feedline run between the facility fill interface and the tank itself. The *CTLVLV* connector is calibrated to flow a set amount of LOX at a given delta pressure. Without an analysis of complete system flow dynamics, the split in LOX flow between the tank and feedlines during chilldown is not known. For modeling purposes, three different loading profiles were used to simulate tank chilldown.

Loading Profiles:

A) Initial Target Flowrate 5 lbm/sec, replenish at 5 lbm/sec
B) Initial Target Flowrate 7 lbm/sec, replenish at 5 lbm/sec
C) Initial Target Flowrate 10 lbm/sec, replenish at 5 lbm/sec

The tank is initially filled at one of these target flowrates and then replenished at 5 lbm/sec as needed in order to keep the tank liquid volume within a –0/+1% band of the nominal fill volume. The tank is constantly vented during the analysis.

The tank vent path consists of one junction upstream and one junction downstream of the vent valve, which is also modeled using a *CTLVLV* macro. A plenum set at ambient pressure (12.7 psia) is used as the ultimate downstream boundary. Different Cd and Cv values may be input in order to model valve flow characteristics. Critical flow through the vent valve is monitored and modeled using FLUINT's *CHOKER* subroutine. Two different valve sizes were examined in this analysis. The valve characteristics are given in Table 3.

Diameter	Cd	Cv
0.5"	0.6	7.1
1.0"	0.7	15.7

Table 3: Valve characteristics

The fluid submodel is shown in Figure 8.

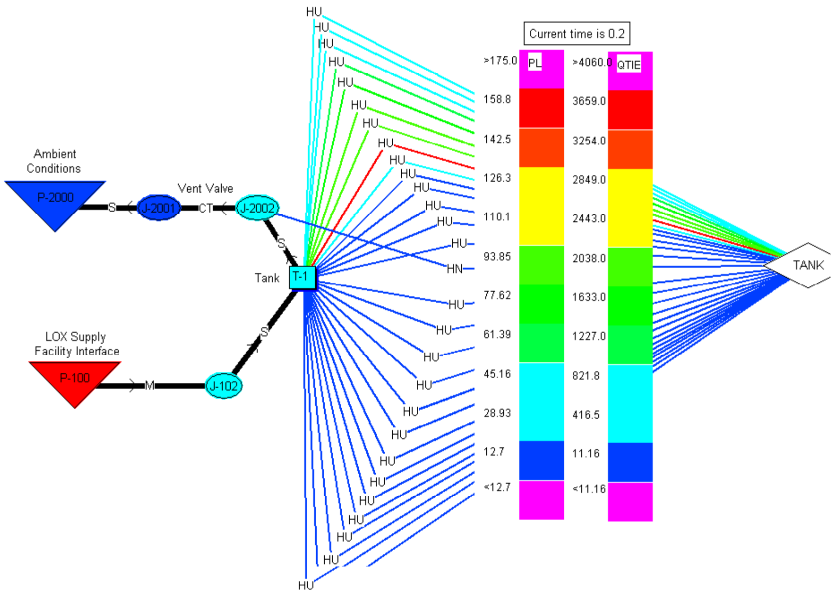

Figure 8: LOX Tank fluid submodel

The tank sphere thermal submodel consists of 28 diffusion nodes. The nodes can be visualized as vertically stacked bands of tank metal with heights set by an arc angle of 6º (except for the bottom and top nodes, which are 12º). The tank nodes are used to capture the vertical temperature gradient established by the ingress of cold fluid at the bottom of the tank and the exit of vapor at the top of the tank. Additionally, 56 arithmetic nodes are used to model the gradient between the tank outer and inner surfaces. This radial gradient is set up by the imbalance of convection heat transfer on the inner wall and radiation heat transfer on the outside wall. A single diffusion node is used to model the thermal mass of the vent line at the top of the tank. Heat leaks due to support struts, liquid-level sensors, pressurization ports, and TVS ports are imposed on the tank shell. Radiation heat transfer to the outer tank shell is calculated through the use of an apparent thermal conductivity value for 100 layers of MLI. The tank thermal model is shown in Figure 9, the orientation is tank bottom-to-top/figure left-to-right.

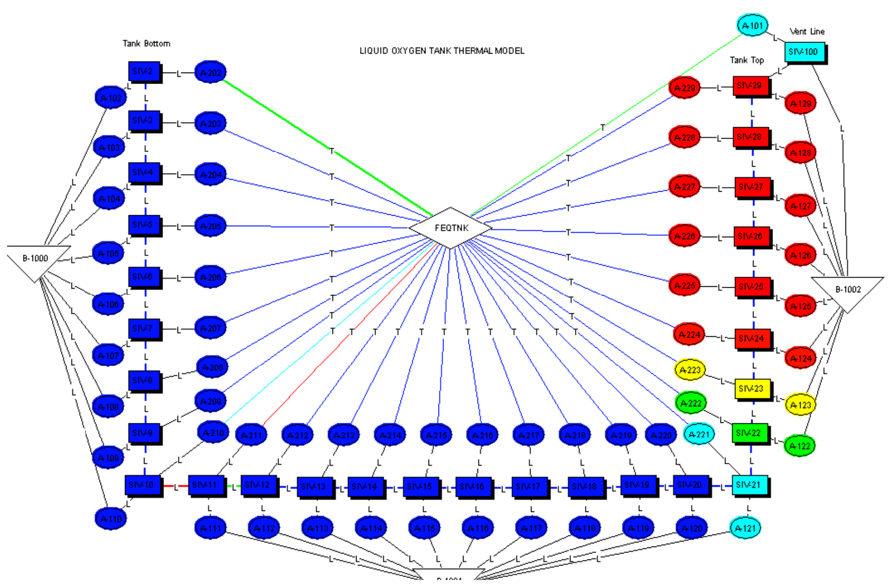

Figure 9: LOX Tank thermal submodel

A series of heat transfer ties connect the fluid and thermal submodels. Heat transfer is handled separately in the three distinct regions of the fluid model: the liquid-filled portion, the ullage, and the vent line. A single film coefficient is calculated for each region using an average temperature of the wall in contact with each region.

Heat is transferred through boiling in the liquid-filled portion of the tank. During the chilldown of cryogenic equipment, the heat transfer process goes through several regimes of boiling due to the large initial excess temperature, ΔT_{excess}. The excess temperature is the difference between the wall boundary temperature, T_{wall}, and liquid saturation temperature, T_{sat}:

$$\Delta T_{excess} = T_s - T_{sat} \tag{3}$$

The excess temperature will decrease as the tank is chilled and as system pressure rises.

Film boiling occurs in systems with large ΔT_{excess}. The correlation of Berenson [3] is used to model convection heat transfer through the film layer.

$$Nu_B = 0.425\left[(Ra/Ja)Bo^{1/2}\right]^{1/4} \tag{4}$$

Radiation heat transfer from the tank wall through the film to the liquid is also considered in this regime:

$$q''_R = \varepsilon\sigma\left(T_s^4 - T_l^4\right) \tag{5}$$

Film coefficients for boiling, h_B, and radiation, h_R, are extracted from Equations 4 & 5 and an overall film coefficient is approximated (Bromley) [4]:

$$h = h_B + 0.750 h_R \tag{6}$$

The heat flux decreases with decreasing excess temperature in the film boiling regime. A minimum heat flux is eventually reached and the heat transfer enters the transition regime. The minimum heat flux is set by (Zuber and Berenson) [3]:

$$q''_{\min} = 0.09\rho_v h_{fg}\left[\frac{g\sigma(\rho_l - \rho_v)}{(\rho_l + \rho_v)^2}\right]^{1/4} \tag{7}$$

The minimum heat flux is reached in the model at an excess temperature of ~35ºR for ambient oxygen. Once ΔT_{excess} falls below this critical point, the boiling transitions. The heat flux starts to rise, with decreasing ΔT_{excess} as more liquid comes in contact with the tank wall. As ΔT_{excess} drops, a maximum heat flux is eventually reached (Kutateladze) [1]:

$$q''_{\max} = 0.149\rho_v h_{fg}\left[\frac{g\sigma(\rho_l - \rho_v)}{\rho_v^{\,2}}\right]^{1/4} \tag{8}$$

The ΔT_{excess} corresponding to the critical heat flux in the model is ~20ºR for ambient oxygen. During transition boiling, the film coefficient is approximated in the tank model via linear interpolation between q''_{min} and q''_{max}.

The heat transfer process transitions to the nucleate boiling regime as ΔT_{excess} continues to decrease past the critical point. Rohsenow's correlation is used for the nucleate boiling regime [4]:

$$q''_B = \mu_l h_{fg}\left[\frac{g(\rho_l - \rho_v)}{\sigma}\right]^{1/2} x \left(\frac{c_{p,l}\Delta T_{excess}}{0.013 h_{fg} \Pr_l^{1.7}}\right)^3 \tag{9}$$

A fourth boiling regime, free convection boiling, is entered as ΔT_{excess} falls below ~2 ºR. The chilldown model does not exhibit much time in the free convection boiling regime, for this reason and in order to smooth the heat transfer calculations, the Rohsenow correlation is used in the limit as ΔT_{excess} goes to zero.

Heat transfer from the tank to the ullage of the tank is modeled as the sum of a free and forced convection calculation. The free convection contribution is calculated using Equation 1 and the Dittus-Boelter correlation is used to model forced convection [1]:

$$Nu = 0.023 \, \mathrm{Re}^{4/5} \, \mathrm{Pr}^{2/5} \tag{10}$$

Heat transfer to the tank vent line is calculated by simply using the Dittus-Boelter correlation of Equation 9.

Tank Model Results & Analysis

A series of six chilldown analysis runs were made using the two vent valve sizes, three loading profiles, and the heat transfer characteristics of the full boiling curve (FBC). Output typical of a modeling run is plotted in Figure 10.

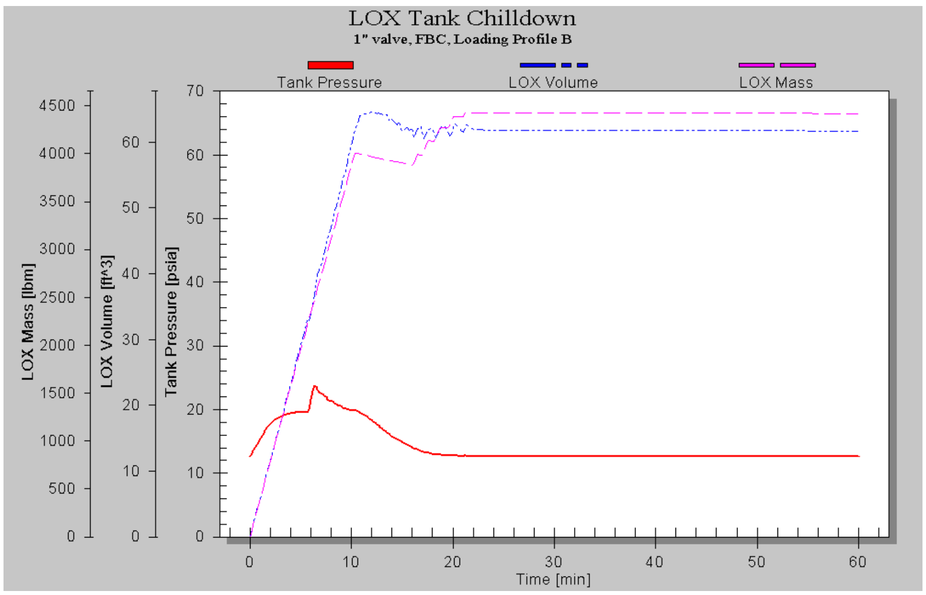

Figure 10: Tank Chilldown Output

Figure 10 shows the tank pressure, liquid volume, and liquid mass for the 1" vent valve, loading profile B, full boiling curve case. Tank pressure rises steadily from the start as the tank begins to fill and film boiling occurs. At about 5:40 (min:sec) into chilldown, the boiling process starts to transition and tank pressure rises as liquid boiling heat flux increases steeply. The critical heat flux is reached at 6:20, coinciding with the peak tank pressure of 23.8 psia, and the tank chills by nucleate boiling for the rest of the run. A slight kneel in pressure is exhibited as the fill valve is closed at 10:20. The average fillrate during the initial fill is 6.46 lbm/sec, slightly less then the target value due to the fill valve calibration method and increased tank pressure. LOX continues to boil-off after the fill valve is closed as exhibited by the downward slope in LOX mass in Figure 10. In the 5 min and 45 sec between initial fill valve closure and reopening for replenishment, 127 lbm of LOX boils off. The tank is then continually topped-off (5 lbm/sec) as needed until the tank is loaded at 21:14 after 5 replenishment cycles. Thermal submodel nodal temperatures are plotted in Figure 11. The lower nodes are cooled before upper nodes as fluid enters the bottom of the tank. Node temperatures drop off abruptly as the adjacent wall is wetted with LOX.

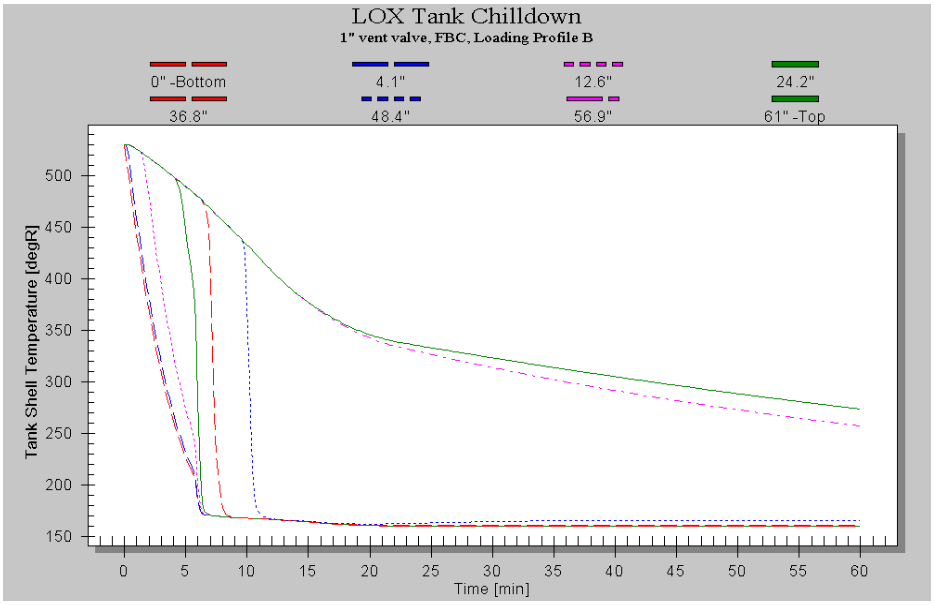

Figure 11: Tank Wall Temperatures

The effect of varying the loading profile was found to be fairly insignificant in terms of tank pressure. The peak pressures associated with the initial fill transient did not vary more than 4.6 psi. The pressure traces for each loading profile are shown in Figure 12 for the 0.5" valve using the full boiling curve. The rigidity in the pressure fall-off during nucleate boiling is due to the liquid volume reattaching to the discrete nodes (all at different temperatures) as liquid level changes.

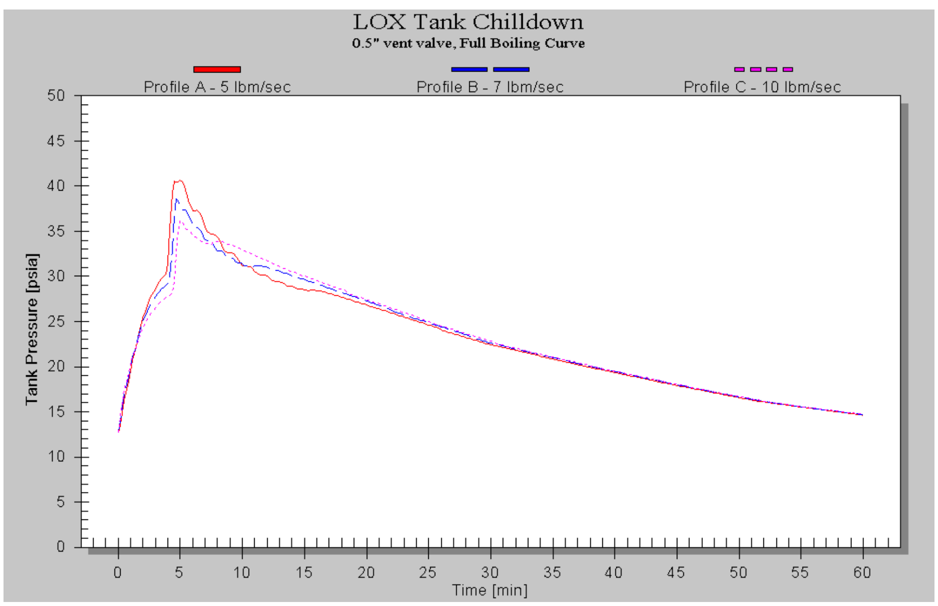

Figure 12: Pressure Variation in Loading Profiles

All modeling runs performed indicated that chilldown and loading of the LOX tank could be accomplished in less than one hour.

In order to adequately bound the maximum pressure rise expected, the previous runs were also made using a maximum heat flux calculation for ΔT_{excess} anywhere above the critical point. This limiting critical heat flux method is denoted in figures and tables as QMAX. Pressure data from a comparison of loading profile B is shown in Figure 13. The maximum pressures and vent rates are given in Table 4 for all model runs performed.

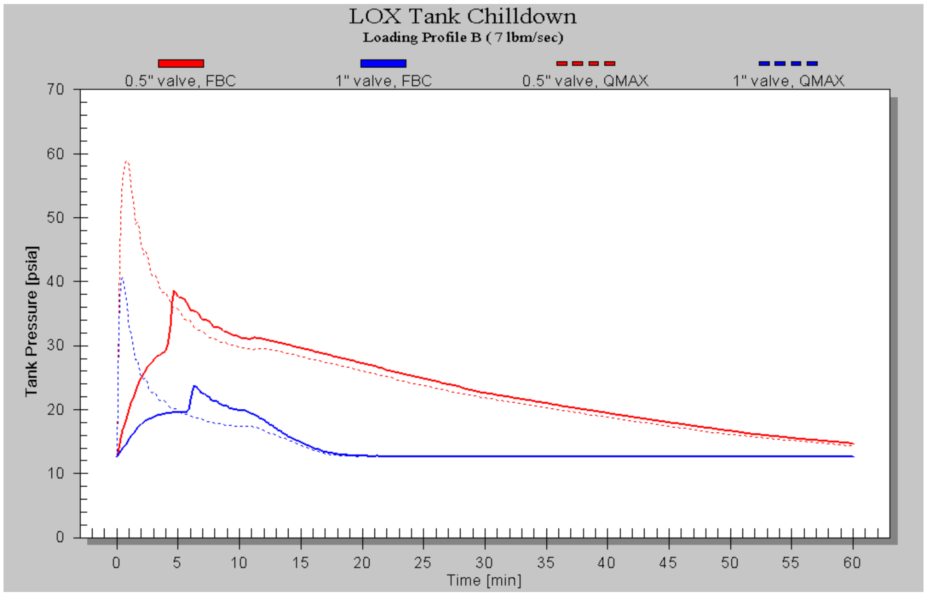

Figure 13: Pressure Variation in Heat Transfer Calculation Method

Valve Size	Heat Transfer Method	Loading Profile	Maximum Pressure (psia)	Maximum Vent Rate (lbm/sec)
0.5"	FBC	A	40.7	0.146
		B	38.6	0.140
		C	36.1	0.136
	QMAX	A	58.4	0.201
		B	59.0	0.203
		C	56.7	0.194
1.0"	FBC	A	22.6	0.424
		B	23.8	0.459
		C	25.1	0.526
	QMAX	A	38.5	0.677
		B	40.6	0.720
		C	41.5	0.740

Table 4: Variation in Maximum Values

The maximum pressure during chilldown as indicated by the model is 59.0 psia. This pressure is well below the nominal operating tank pressure of 350 psia. The highest vent rates for each valve were 0.203 lbm GOX/sec for the ½" valve and 0.740 lbm GOX/sec for the 1" valve.

Conclusions

Modeling and analysis have established the feasibility of meeting the one-hour requirement to chill and fill the NT-APS-TB liquid oxygen tank and feedsystem. Analysis of the accumulator thermal design has determined that it is more beneficial with respect to system chilldown time to orient the accumulator such that the LOX side is above the GHe ullage. This orientation augments heat transport from end-to-end via free convection. Thermal modeling of the accumulator indicates that the accumulator will load up within one hour. Modeling of the LOX tank shows no issues with chilling and filling the propellant tank with a full load of LOX within one hour. Large pressure rises in the tank during boiling were not an issue even for the smaller vent valve.

References

[1] Incropera, F.P., and D.P. Dewitt. 1996. *Introduction to Heat Transfer*. 3rd ed. New York: John Wiley and Sons.

[2] Kays, W.M. and M.E. Crawford. 1993. *Convective Heat and Mass Transfer*. 3rd ed. New York: McGraw –Hill Book Company.

[3] Berenson, P.J., 1961. Film boiling heat transfer from a horizontal surface. *Journal of Heat Transfer,* 83:351-358.

[4] Barron, R.F. 1999. *Cryogenic Heat Transfer*. Philadelphia: Taylor & Francis.